CONDUCTIVITY OF $CsPbBr_3$ AT AMBIENT CONDITIONS

L.-I. I. Bulyk[1,2], O. T. Antonyak[1], Ya. M. Chornodolskyy[1], R. V. Gamernyk[1], T. M. Demkiv[1], V. V. Vistovskyy[1], A. Suchocki[2], A. S. Voloshinovskii[1]

[1] *Ivan Franko National University of Lviv, 8, Kyrylo & Mefodiy St., Lviv, Ukraine*

[2] *Institute of Physics, Polish Academy of Sciences, Al. Lotników 32/46, 02-668, Warsaw, Poland*

e-mail: tmdemkiv@gmail.com

(Received 20 August 2021; in final form 10 November 2021; accepted 22 November 2021; published online 22 December 2021)

The properties of electrically conductive $CsPbBr_3$ single crystals obtained from the melt have been studied. According to the results of Raman spectra, the covalent bonds in the octahedra $[PbBr_6]^{4-}$ have different strengths in different directions. This bond anisotropy promotes the formation of bromine vacancies located along selected crystallographic directions, which become sites of crystal degradation and the formation of Cs_4PbBr_6 microformations. A potential barrier at the boundary between the Cs_4PbBr_6 single crystal and the Cs_4PbBr_6 microformations was found.

Key words: single crystal, electrically conductive, Raman spectra, voltage-current characteristics, microformations.

DOI: https://doi.org/10.30970/jps.25.4801

I. INTRODUCTION

In recent years, inorganic halide perovskites have attracted much attention from scientific community. These materials have promising properties for use in emitting and recording diodes [1], as laser-active media [2], as photosensitive elements for solar cells [3], etc. Such a wide field of application is related to appropriate properties and the ability to control them in a wide range of values. For example, the exciton luminescence of inorganic halogen perovskites $CsPbX_3$, where $X = \mathrm{I, Cl, Br}$ [4], and their mixtures cover the entire visible part of the spectrum.

$CsPbBr_3$ crystals exhibit a high quantum luminescence yield with a narrow luminescence exciton band [5]. Furthermore, the halide change in perovskite allows one to smoothly shift the edge of its absorption and the radiation band in a wide range from UV to red. These properties make them promising when used as phosphors to form a color image. In addition, during the transition from a single bulk crystal to nanocrystals, a change in the wavelength of emission is observed due to the quantum size effect [4].

With a temperature change, perovskites undergo phase transitions. In particular, $CsPbBr_3$ transforms from the cubic to the tetragonal phase at 132°C and from the tetragonal to the orthorhombic phase at 78°C. For nanoscale $CsPbBr_3$, the coexistence of tetragonal ($P4/mbm$) and orthorhombic ($Pbnm$) phases at temperatures below room temperature was detected. Another phase transition from the orthorhombic to the tetragonal phase was registered at room temperature under illumination [7]. The conversion of $CsPbBr_3$ to the Cs_4PbBr_6 phase was registered in [8] under the moisture influence on the sample. Thus, at different temperatures, $CsPbBr_3$ may be in different phases, as well as it can contain inclusions of different phases simultaneously. The electrical current contributes to the degradation of crystals due to the ionic nature of the conductivity in this material.

The conductive properties of perovskites depend on the method of crystal synthesis. This is because the synthesis determines the quality of the samples, the structure, and the number of defects in the lattice [9]. Therefore, a profound understanding of the sample structure and the nature of sample defects is crucial. It will help to effectively use the merits of these materials and minimize the impact of degradation on their properties [10].

II. TECHNIQUE, METHODOLOGY AND SAMPLE PREPARATION

The synthesis of $CsPbBr_3$ was performed in a quartz ampoule of CsBr and $PbBr_2$ of high purity, mixed in a stoichiometric ratio. $CsPbBr_3$ single crystals were grown by the Stockbarger method. Samples for the study were chopped from the grown big crystal. During the chipping of the samples, a plane of easy-cleavage ($[x]$-slice in Fig. 1,b) was found. The sample splits much easier along this plane than in the direction perpendicular to it ($[z]$-slice). The poorly chipped surfaces of the sample ($[z]$-slice in Fig. 1) were polished with Al_2O_3 powder with a grain size of 1–10 μm.

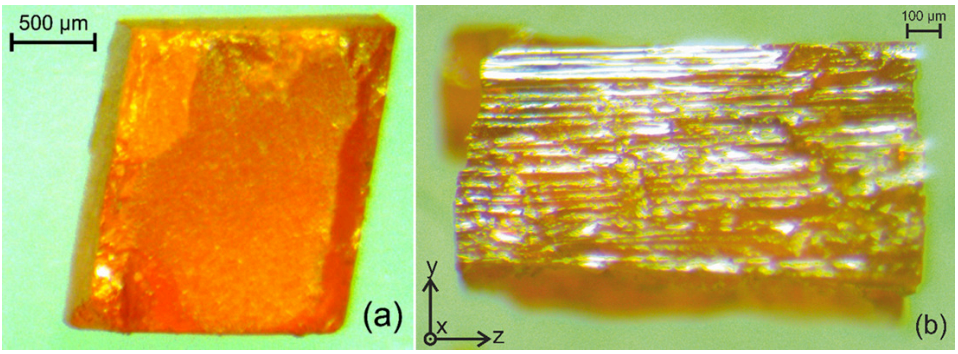

Fig. 1. Sample $CsPbBr_3$: a) $[z]$-slice (polished), b) — $[x]$-slice (chopped)

For electrical measurements, silver paste contacts were made on the chipped planes of the $[x]$ and $[y]$-slices or on the polished surface of the $[z]$-slice of the sample. The sample dimensions were determined using an optical microscope.

The structure identification and sample quality were evaluated with the use of Raman spectra. A 785 nm laser was used for excitation in Raman experiments. The spectra were obtained using a computer-controlled Monovista CRS + (SI Ltd) set-up with a Trivista Software.

The resistance of the samples was measured using KEITHLEY 6517B electrometer. The DC voltage source built into the electrometer was used to apply voltage to the sample with the 5 mV increment. The measurement was performed with an automatic system using a program written in LabView. The first measurement of voltage-current characteristics of polished and chipped samples was performed immediately after chipping and polishing and preparation of contacts. Subsequent measurements were repeated every two days for two weeks.

During the photoconductivity measurements, $CsPbBr_3$ was excited by an SLD-405-100T semiconductor laser with a radiation wavelength of 405 nm and a nominal power of 100 mW. Normally the laser beam fell on the sample surface perpendicular to the direction of the passing current, without illuminating the contacts. The change in the laser irradiation power of the sample was provided by a set of glass neutral-density filters.

III. RESULTS

Raman spectra measured under 785 nm laser excitation are given in Fig. 2. A narrow line at 72 cm^{-1} and broadband in the range 127–175 cm^{-1} are observed for all samples. These lines correspond to the oscillatory modes of the pair of Cs^+ cations and $[PbBr_6]^{4-}$ octahedra. The peak at 310 cm^{-1} (inset in Fig. 2) corresponds to the second-order of the oscillating band of the octahedron $[PbBr_6]^{4-}$ [9, 10]. As it can be seen, a band around 127 cm^{-1} has a relatively lower intensity in the Raman spectrum of the polished sample than in the chopped samples.

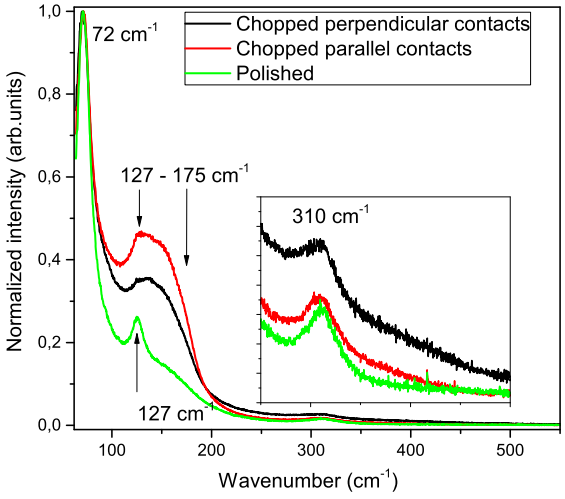

Fig. 2. Raman spectra of $CsPbBr_3$ excited at 785 nm for chopped and polished samples

Voltage-current characteristics in three different directions of current for the sample $CsPbBr_3$ are presented in Fig. 3. The average values of resistivity were: in the direction Ox — 0.76 GΩ·cm, in the direction Oy — 0.44 GΩ·cm. In both cases, current density is almost independent of time (see Fig. 3,a,b). The voltage-current characteristic in the Oy direction is more linear (see Fig. 3,a,b) than in the Ox direction. On the contrary, the scatter of the conductivity values is larger for the Oy direction than in the Ox direction. In the case of Oz direction (contacts on polished surfaces), the voltage-current characteristic is linear only during the first 10 to 20 hours (see Fig. 3,c). During the week it loses linearity after longer measurements. In particular, at the electrical field strengths below 0.3 V/cm, the current decreases and almost does not depend on the electrical field. With the field around 0.5 V/cm, current comes back to the level of linear characteristics which were observed during the first 20 hours. Before the linearity loss, the average value of resistivity was 0.65 GΩ·cm. The obtained values of resistivity are in good agreement with the results obtained by other authors [12–14].

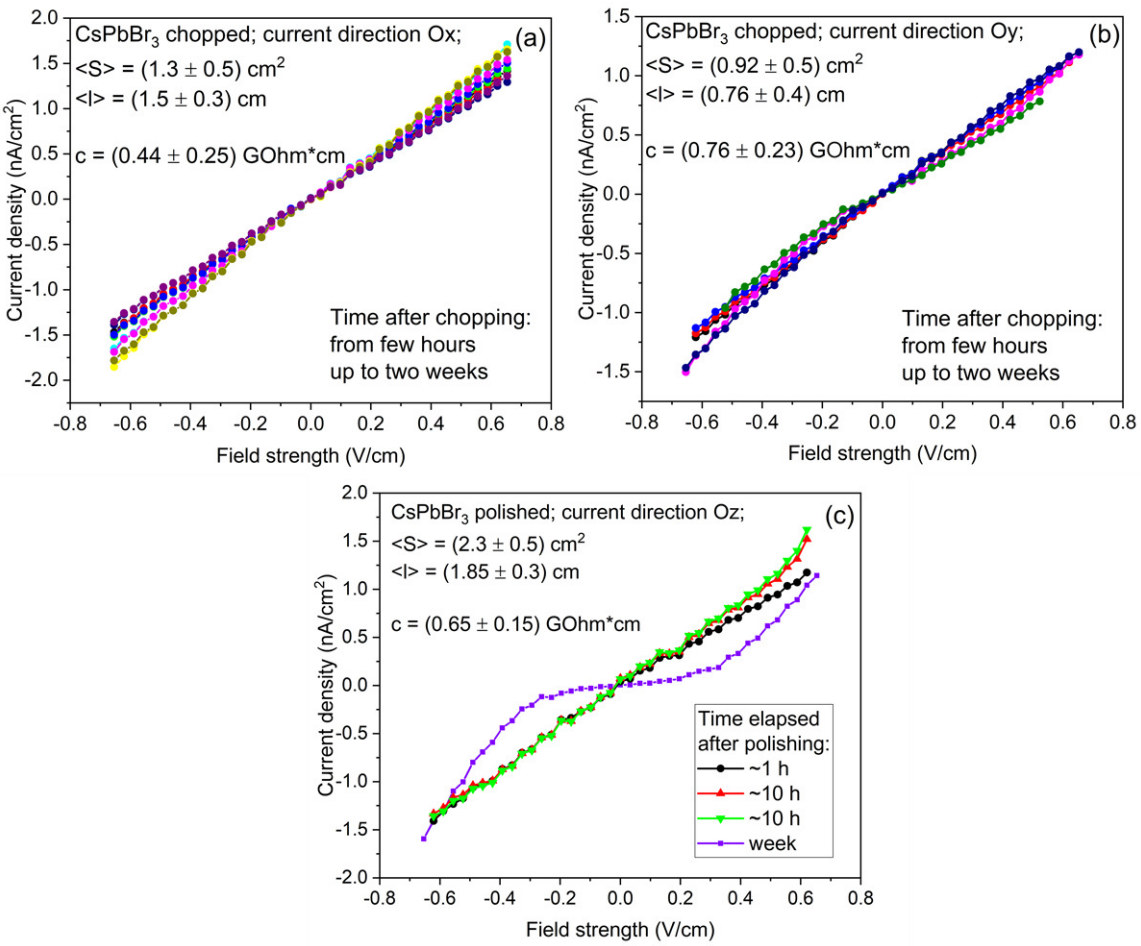

Fig. 3. Voltage-current characteristics of $CsPbBr_3$ crystal for three different current directions: a — chopped sample (current direction Ox); b — chopped sample (current direction Oy); c — polished sample (current direction Oz)

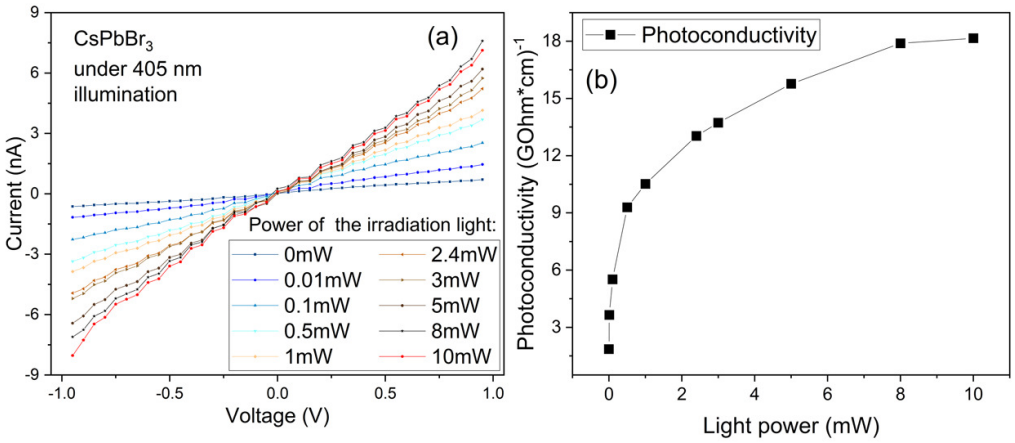

Fig. 4. Photoconductivity of $CsPbBr_3$ excited by a laser with a wavelength of 405 nm

In Fig. 4,a, the voltage-current characteristics of $CsPbBr_3$ during its irradiation with a semiconductor laser with a wavelength of 405 nm are shown. As can be seen from the graph, as the intensity of the irradiating light increases, the resistance of the sample decreases. Also, there is a slight nonlinearity of the voltage-current characteristics of the illuminated sample. Figure 4,b shows the photoconductivity dependence on irradiation power, which illustrates the saturation tendency.

IV. DISCUSSION

Due to the phase transition [12, 15] from the cubic to the tetragonal phase (which occurs at 132°C), the octahedra $[PbBr_6]^{4-}$ alternately rotate around the crystallographic axis of the fourth-order. During the transition from the tetragonal to the orthorhombic phase (occurs at 87°C), the rotation increases, and additional deformation of octahedra $[PbBr_6]^{4-}$ occurs [2]. As a result, the length of the Pb–Br bond becomes different, and the rhombuses formed alternately rotate. This deformation causes different strengths of the Pb–Br covalent bond. This is confirmed by the wide structural contour of the Raman scattering band from the X and Y planes in the range 127–175 cm^{-1} [16, 17], which is the result of oscillations of different frequencies, and confirms the different distances between Pb^+ and Br^- ions. Therefore, Br^- sites become unequal, which may be the reason for forming bromine vacancies located in selected crystallographic directions. The existence of such bromine vacancies reduces the integrity of the crystal and causes additional anisotropy of the physical properties of the crystal [18]. Such directions can form planes of quasi-cleavage. In addition, bromine vacancies located in selected crystallographic directions may be the sites of other phases formation, in particular Cs_4PbBr_6. In our study, the 127 cm^{-1} line is clearly distinguished in the Oz direction, confirming the deformation of the octahedra $[PbBr_6]^{4-}$ in only two directions Ox and Ox. Some authors, in particular in [19], claim that a narrow band of 127 cm^{-1} is characteristic of Cs_4PbBr_6. Therefore, the presence of a band of 127 cm^{-1} in the Raman spectra requires additional discussion

Oriented microformations of Cs_4PbBr_6 will reduce the conductivity of the crystal in the Ox and Oy directions. Furthermore, due to mechanical treatment during polishing, an amorphous layer is expected to form on the surface. Therefore, the resistance in the Oz direction is higher due to the application of contacts on those polished surfaces. In addition, the concentration of Cs_4PbBr_6 formations in the amorphous layer may increase over time, which, obviously, may cause the increased nonlinearity of the voltage-current characteristics of $CsPbBr_3$ (Fig. 3,c).

V. CONCLUSIONS

Raman scattering studies indicate that the magnitude of Pb–Br covalent bonds is different in different directions. As a result, Br anions become unequal, and this is the reason for the formation of bromine vacancies located in selected crystallographic directions. This process leads to the appearance of quasi-cleavage planes, degradation of the crystal structure of $CsPbBr_3$ due to microformations of Cs_4PbBr_6. This is manifested in the change of the spectra of Raman scattering and in voltage-current characteristics, i.e the appearance of a band of 127 cm^{-1} and emergence of nonlinearity of the voltage-current characteristic caused by a potential barrier between the $CsPbBr_3$ single crystal and Cs_4PbBr_6 microformations, respectively.

[1] X. Mo *et al.*, Nanoscale **11**, 21386 (2019); https://doi.org/10.1039/c9nr06682a.

[2] X. Zhang, F. Wang, B. Bin Zhang, G. Zha, W. Jie, Cryst. Growth Des. **20**, 4585 (2020); https://doi.org/10.1021/acs.cgd.0c00370.

[3] H. Li, Q. Wei, Z. Ning, Appl. Phys. Lett. **117**, 060502 (2020); https://doi.org/10.1063/5.0014804.

[4] M. V. Kovalenko, M. I. Bodnarchuk, Chimia: Int. J. Chem. **71**, 461 (2017); https://doi.org/10.2533/chimia.2017.461.

[5] M. Dendebera *et al.*, J. Lumin. **225**, 117346 (2020); https://doi.org/10.1016/j.jlumin.2020.117346.

[6] T. J. Whitcher *et al.*, NPG Asia Mater. **11**, 70 (2019); https://doi.org/10.1038/s41427-019-0170-6.

[7] J. Xue *et al.*, Adv. Funct. Mater. **29**, 13, 1807922 (2019); https://doi.org/10.1002/adfm.201807922.

[8] B. Akbali, G. Topcu, T. Guner, Phys. Rev. Mater. **2**, 034601 (2018); https://doi.org/10.1103/PhysRevMaterials.2.034601.

[9] J. H. Cha *et al.*, J. Phys. Chem. Lett. **8**, 565 (2017); https://doi.org/10.1021/acs.jpclett.6b02763.

[10] L.-I. Bulyk *et al.*, J. Alloys Compd. **884**, 161023 (2021); https://doi.org/10.1016/j.jallcom.2021.161023.

[11] O. Yaffe *et al.*, Phys. Rev. Lett. **118**, 136001 (2017); https://doi.org/10.1103/PhysRevLett.118.136001.

[12] M. Zhang *et al.*, J. Cryst. Growth **484**, 37 (2018); https://doi.org/10.1016/j.jcrysgro.2017.12.020.

[13] M. I. Saidaminov *et al.*, Adv. Opt. Mater. **5**, 1600704 (2017); https://doi.org/10.1002/adom.201600704.

[14] H. Zhang *et al.*, Cryst. Growth Des. **17**, 6426 (2017); https://doi.org/10.1021/acs.cgd.7b01086.

[15] S. Svirskas *et al.*, J. Mater. Chem. A **8**, 14015 (2020); https://doi.org/10.1039/d0ta04155.

[16] L. Zhang, Q. Zeng, K. Wang, J. Phys. Chem. Lett. **8**, 3752 (2017); https://doi.org/10.1021/acs.jpclett.7b01577.

[17] C. Wang *et al.*, Adv. Mater. **31**, 1902492 (2019); https://doi.org/10.1002/adma.201902492.

[18] Z. Ma *et al.*, Nat. Commun. **9**, 4506 (2018); https://doi.org/10.1038/s41467-018-06840-8.

[19] Z. Qin *et al.*, Chem. Mater **31**, 9098 (2019); https://doi.org/10.1021/acs.chemmater.9b03426.

ПРОВІДНІ ВЛАСТИВОСТІ $CsPbBr_3$ ЗА НОРМАЛЬНИХ УМОВ

Л.-І. І. Булик[1,2], О. Т. Антоняк[1], Я. М. Чорнодольський[1], Р. В. Гамерник[1], Т. М. Демків[1], В. В. Вістовський[1], А. Сухоцький[2], А. С. Волошиновський[1]

[1] *Львівський національний університет імені Івана Франка, вул. Кирила і Мефодія, 8, Львів, 79005, Україна,*

[2] *Інститут фізики, Польська Академія наук, Варшава, Польща*

e-mail: tmdemkiv@gmail.com

Досліджено електропровідні властивості (вольт-амперні характеристики та фотопровідність під дією напівпровідникового лазера з довжиною хвилі випромінювання 405 нм) монокристалів $CsPbBr_3$, отриманих із бінарних сполук CsBr і $PbBr_2$ високої чистоти, змішаних у стехіометричному співвідношенні, методом Стокбарґера. Виміряні під час збудження лазерним випромінюванням з $\lambda = 785$ нм раманівські спектри показали наявність вузької лінії за 72 $см^{-1}$ та широкої смуги в діапазоні 127–175 $см^{-1}$, які відповідають коливальним модам пари октаедрів Cs в оточенні Br та октаедрів $[PbBr_6]^{4-}$ відповідно. Пік за 310 $см^{-1}$ відповідає другому порядку коливальної смуги октаедра $[PbBr_6]^{4-}$. Це проявляється в зміні спектрів комбінаційного розсіювання світла — виникнення смуги 127 $см^{-1}$, що підтверджує деформацію октаедрів $[PbBr_6]^{4-}$ лише у двох напрямках — X та Y, яка приводить до різної величини ковалентного зв'язку Pb–Br в октаедрах $[PbBr_6]^{4-}$. Така анізотропія зв'язків сприяє утворенню орієнтованих у певних виділених напрямках вакансій брому, які стають місцями деґрадації кристала та виникненню мікроутворень Cs_4PbBr_6 і приводить до появи площин квазіспайності та деґрадації кристалічної структури $CsPbBr_3$ унаслідок виникнення мікроутворень Cs_4PbBr_6. На межі монокристала $CsPbBr_3$ та мікроутворень Cs_4PbBr_6 виявлено потенціальний бар'єр, який проявляється в нелінійності вольт-амперної характеристики $CsPbBr_3$. Вольт-амперна характеристика в напрямку Oy є більш лінійною, проте розкид значень провідності більший, ніж за протікання струму в напрямку Ox. У напрямку Oz (контакти на полірованих поверхнях) вольт-амперна характеристика лінійна лише протягом перших 10–20 годин. Орієнтовані в певних напрямках мікроутворення Cs_4PbBr_6 понижують провідність кристала в напрямках X та Y. Більший опір у Z-напрямку зумовлений нанесенням контактів на полірувані поверхні, на яких є аморфний шар, унаслідок механічної обробки. Крім того, в аморфному шарі з часом додатково може зростати концентрація утворень Cs_4PbBr_6, які, очевидно, і зумовлюють появу нелінійності у вольт-амперній характеристиці $CsPbBr_3$.

Ключові слова: монокристал, електропровідність, спектри КРС, вольт-амперні характеристики, мікроутворення